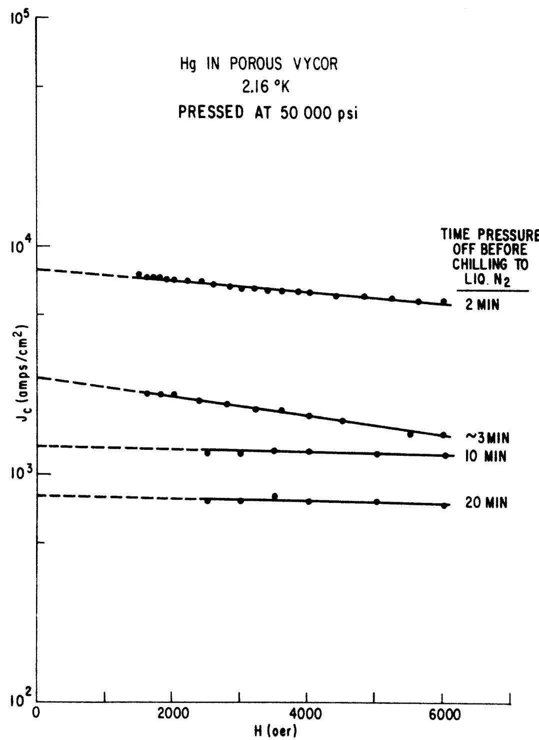

FIG. 2. Critical current densities as a function of field.

tained in this way are shown in Fig. 2.

There are two theories of the enhancement of critical field by small dimensions. The original London[5] theory suggests that this enhancement is on the order of λ_0/R', where λ_0 is the penetration depth, while the modification suggested by Pippard's[6] concept of a coherence length ξ_0 gives the order of $\lambda_0\xi_0^{1/2}/R'^{3/2}$. If λ_0 is taken to be 430 Å, ξ_0 as 2000 Å, and $H_c(2.1°\mathrm{K}) = 320$ oersteds, then the two estimates are ~4600 and ~40 000 oersteds, respectively, for the London and Pippard limits. While we could not go to high enough fields to drive the filaments normal, the Pippard limit appears to have more truth in it than the London limit.

The main conclusion of this note is that artificial structures may be devised that simulate the known high-field, high-current superconductors. In addition to their interest in clarifying the basis of these phenomena, these techniques may be used to prepare specimens for electron or nuclear resonance experiments[7] where the techniques of colloidal particles or thin films are difficult to employ.

We wish to acknowledge the suggestion of R. E. Carter that we use Vycor. In addition, we wish to thank J. W. Borough for carrying out the impregnation of the samples.

[1]K. Mendelssohn, Proc. Roy. Soc. (London) A152, 34 (1935).

[2]A product of Corning Glass Works.

[3]F. A. Schwertz, J. Am. Ceram. Soc. 32, 390 (1949).

[4]C. P. Bean, Phys. Rev. Letters 8, 250 (1962).

[5]F. London, Superfluids (John Wiley & Sons, Inc., New York, 1950), Vol. I.

[6]M. Tinkham, Phys. Rev. 110, 26 (1958).

[7]See, for example, F. Reif, Phys. Rev. 102, 1417 (1956); 106, 208 (1957).

CRITICAL POINTS AND ULTRAVIOLET REFLECTIVITY OF SEMICONDUCTORS*

D. Brust† and J. C. Phillips
Department of Physics, University of Chicago, Chicago, Illinois

and

F. Bassani
Argonne National Laboratory, Argonne, Illinois

(Received June 18, 1962)

The dielectric fine structure of semiconductors in the visible and ultraviolet is determined by direct interband transitions.[1] Neglecting lifetime broadening, the contribution of such transitions to the imaginary part ϵ_2 of the dielectric constant is

$$\epsilon_2(\nu) = \sum_{\vec{k}, n} f(\vec{k}, n)\delta(h\nu - E_{\vec{k}}), \quad (1)$$

where n labels a pair of bands, one valence and one conduction. Here f is the oscillator strength; calculations discussed below show that f is approximately proportional to $C(n)/E^2$, so that

$$\epsilon_2(\nu) = \sum_n \rho_n(h\nu)C(n)/\nu^2, \quad (2)$$

where $\rho_n(E)$ is the joint density of states for energy $E = E_n = E^c - E^v$.

It is known[2] that structure in the reflectance is similar in shape to structure in ϵ_2; from (2) this is determined by structure in ρ_n. According to the critical point theory[3,4] corners in $\rho_n(E)$ occur whenever

$$\vec{\nabla}_k(E_{\vec{k}}^c - E_{\vec{k}}^v) = 0. \quad (3)$$

At symmetry points to which previous analysis was confined $\vec{\nabla}_k E^c = 0$ and $\vec{\nabla}_k E^v = 0$ separately; at more general points of the Brillouin zone one may have $\vec{\nabla}_k E^c = \vec{\nabla}_k E^v$ so that (3) may still hold.

The corners that occur in $\rho_n(E)$ are of two kinds: minima (M_0) and maxima (M_3), or saddle points (M_1 and M_2). The latter tend to occur near peaks in ρ_n whereas the former occur when ρ_n is small. Because of lifetime broadening in room temperature reflectivity data[1] only saddle-point corners have been identified with confidence.

Here we analyze reflectivity data[5] taken at 25°K on Ge and 80°K on GaAs.[6] These data enable us to resolve M_0 corners as well as new saddle-point corners. These corners are predicted by calculations we have carried out using the pseudopotential[7] parameters for Ge of Bassani and Celli.[8] The calculations used a basis set of about 50 plane waves. They were carried out at about 50 000 points in the Brillouin zone in order to obtain good statistics for a histogram (energy interval 0.1 eV) approximation to $\rho_n(E)$. The pseudopotential values for the squared interband momentum matrix elements [denoted by $C(n)$] are found to be approximately $\vec{k}$-independent.

The theoretical calculation of ϵ_2 from (2) is shown in Fig. 1, which also gives the experimental curve[2] for ϵ_2. It is found that most of the resolved structure comes from $(4 \rightarrow 5)$ and $(4 \rightarrow 6)$ transitions. The energies associated with the corners in Fig. 1 are tabulated and compared with experiment in Table I, which gives a description of the critical points involved. The various interband transitions are shown in Fig. 2.

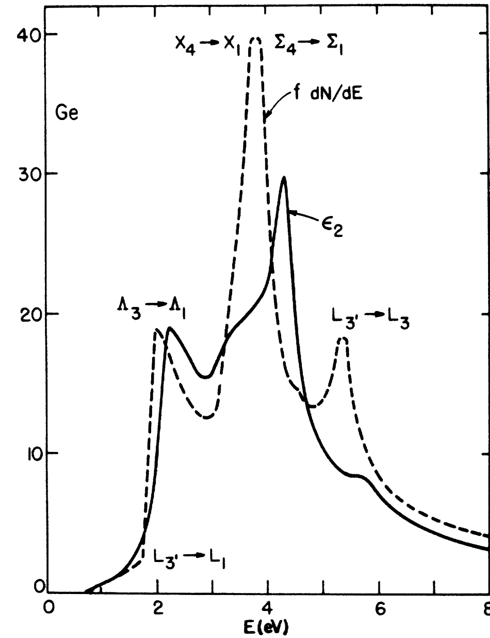

FIG. 1. The joint density of states dN/dE for interband transitions, weighted by oscillator strength f, is compared with the experimental ϵ_2 for Ge. The normalization of the theoretical curve has been adjusted to agree with the experimental curve near 2 eV.

Several features of these results deserve special comment. The large M_1 edges[5] at 2.26 ± 0.02 eV and 2.44 eV in Ge, previously attributed to $L_{3'} \rightarrow L_{1'}$, are now assigned to $\Lambda_3 \rightarrow \Lambda_1$, while $L_{3'} \rightarrow L_1$ is assigned to the M_0 thresholds at 2.02 ± 0.04 eV and 2.18 ± 0.03 eV. According to Roth,[9] the longitudinal g shift for conduction electrons at L_1 is

$$g_{\parallel} = -\left(\frac{m}{m_t} - 1\right)\frac{\Delta_{so}}{\langle E_{L_1} - E_{L_{3'}}\rangle}. \quad (4)$$

Table I. Important critical points in interband transitions below 6 eV are tabulated and classified. An exhaustive list will be given elsewhere.

Type	Location	Bands	Symbol	Theo. Energy	Exper. Energy
M_0	(0,0,0)	$4 \rightarrow 5$	$\Gamma_{25'} \rightarrow \Gamma_{2'}$	0.6	0.8
M_0	(0.5,0.5,0.5)	$4 \rightarrow 5$	$L_{3'} \rightarrow L_1$	1.8	2.1
M_1	(0.17,0.17,0.17)	$4 \rightarrow 5$	$\Lambda_3 \rightarrow \Lambda_1$	2.0	2.3
M_1	(1.0,0,0)	$4 \rightarrow 5$	$X_4 \rightarrow X_1$	3.6	4.3
M_2	(0.61,0.61,0)	$4 \rightarrow 5$	$\Sigma_4 \rightarrow \Sigma_1$	3.8	4.4
M_0	(0,0,0)	$4 \rightarrow 6$	$\Gamma_{25'} \rightarrow \Gamma_{15}$	3.6	3.2
M_1	(0.56,0.56,0.39)	$4 \rightarrow 6$	...	5.3	5.6
M_2	(0.5,0.5,0.5)	$4 \rightarrow 6$	$L_{3'} \rightarrow L_3$	5.4	5.7

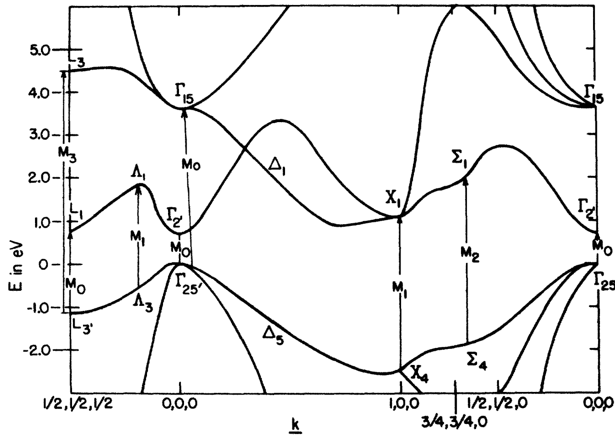

FIG. 2. Pseudopotential energy bands along the (100), (111), and (110) axes for Ge. Important critical points in the interband transitions are indicated.

Taking $\Delta_{SO} = 0.18$ eV, agreement with experiment, $\delta g_{\parallel} = -1.13$, is materially improved by using for the average $\langle E_{L_1} - E_{L_{3'}} \rangle = 2.1$ eV instead of 2.35 eV.

According to Ge-Si alloy data[10] $\Lambda_1 - \Lambda_3 = 3.6$ eV in Si. Because $(\Lambda_1 - \Lambda_3) - (L_1 - L_{3'}) = 0.25$ eV in Ge, the threshold at 3.25 eV in Si may reasonably be assigned to $L_{3'} \rightarrow L_1$.

Our theoretical calculations also explain the line shape of the largest peak near 4 eV. It results from the near degeneracy (separation 0.1 eV) of an M_2 saddle point at $\vec{k} = (0.6, 0.6, 0.0)$ with an M_1 saddle point at $\vec{X} = (100)$.

The results shown in Figs. 1 and 2 do not include spin-orbit effects. In the case of twofold degeneracies or quasi-degeneracies if Δ_{SO} is smaller than the difference between critical point energies, a doubling of the structure results from inclusion of spin-orbit interaction (e.g., $L_{3'} \rightarrow L_1$ and $\Lambda_3 \rightarrow \Lambda_1$ in Ge). Threefold degeneracies are split into $J = \frac{3}{2}$ and $J = \frac{1}{2}$ levels which generally result in a sharpening of the structure (e.g., $\Gamma_{25'}^{3/2} \rightarrow \Gamma_{15}^{1/2}$ and $\Gamma_{15}^{3/2}$).

Novel changes in the joint density of states can be obtained by reversal of the order of critical points when Δ_{SO} is larger than the difference between orbital critical point energies. These changes may explain pseudo-exciton structure[5,11] in CdTe near the $\Lambda_3 \rightarrow \Lambda_1$ edge.

Because of lifetime broadening the M_0 thresholds near 2 eV in Ge are barely resolved although they are well resolved in GaAs.[6] These thresholds appear to be broadened by $\hbar/\tau \sim 0.15$ eV at room temperature and 0.05 eV at 25°K, as expected from Debye ($\theta_D = 300$°K) phonon emission and absorption broadening. At room temperature $\tau \sim 4 \times 10^{-15}$ sec, and with $v = 10^8$ cm/sec, $l = 40$ Å, in good agreement with "hot carrier" estimates[12] for electron mean free paths between phonon emission or absorption.

From Fig. 1 it appears that the lifetime broadening of the L_3 level is much greater, say $\hbar/\tau \sim 1$ eV. This level is about 4.5 eV above the bottom of the conduction band. Presumably the greater broadening is not due to decay by pair production,[12] but to stronger phonon emission and absorption.

The most serious shortcoming of the pseudopotential calculation is the location of the big $X_4 \rightarrow X_1$, $\Sigma_4 \rightarrow \Sigma_1$ peak near 3.8 eV instead of 4.4 eV. Here it overlaps the smaller $\Gamma_{25'} \rightarrow \Gamma_{15}$ transitions, which are calculated to be at 3.6 eV instead of 3.2 eV. Although the peaks are well resolved experimentally, this overlap prevents their being resolved in the total theoretical $f\rho(E)$. For this reason we have calculated each term in (2) separately. The big peak then occurs in the $4 \rightarrow 5$ transitions and the smaller one in $4 \rightarrow 6$ transitions.

Aside from these shortcomings at Γ and X the pseudopotential method interpolates between Γ, X, and L with an accuracy of 0.1 eV. We feel that this is most remarkable for the complicated band structure shown in Fig. 2. Accuracy of this sort requires that the model wave function ϕ contain about 50 plane waves, thereby giving a very accurate treatment of the covalent bond. From an operational viewpoint the positions of three levels within 1 eV above $\Gamma_{25'}$ has been used to predict the entire band structure for

$$-3.6 \text{ eV} < E < +4.0 \text{ eV}, \qquad (5)$$

i.e., a range of nearly 8 eV.

*Work supported in part by the Office of Naval Research and the U. S. Atomic Energy Commission.

†Argonne National Laboratory thesis student.

[1]H. Ehrenreich, H. R. Philipp, and J. C. Phillips, Phys. Rev. Letters 8, 59 (1962).

[2]H. R. Philipp and E. A. Taft, Phys. Rev. 113, 1002 (1959).

[3]L. Van Hove, Phys. Rev. 89, 1189 (1953).

[4]J. C. Phillips, Phys. Rev. 104, 1263 (1956).

[5]D. T. F. Marple and H. Ehrenreich, Phys. Rev. Letters 8, 87 (1962). These authors also point out the importance of a critical point analysis.

[6]D. Greenaway, following Letter [Phys. Rev. Letters 9, 97 (1962)].

[7]J. C. Phillips, Phys. Rev. 112, 685 (1958).

[8]F. Bassani and V. Celli, J. Phys. Chem. Solids 20, 64 (1961).

[9]L. M. Roth, Phys. Rev. 118, 1534 (1960). The use of only one interband term in (4) has been justified by L. Liu, Phys. Rev. 126, 1317 (1962).

[10]J. Taue and A. Abraham, J. Phys. Chem. Solids 20, 190 (1961).

[11]M. Cardona and G. Harbeke, Phys. Rev. Letters 8, 90 (1962).

[12]W. Shockley, in Proceedings of the International Conference on Semiconductor Physics, Prague, 1960 (Czechoslovakian Academy of Sciences, Prague, 1961), Suppl.

FUNDAMENTAL REFLECTIVITY OF GaAs AT LOW TEMPERATURE

D. L. Greenaway
Laboratories RCA Ltd., Zurich, Switzerland
(Received June 20, 1962)

Recent work[1] has shown that the main ultraviolet reflectivity peak in C, Si, and Ge is due to transitions at or near the X point of the Brillouin zone (zone edge, ⟨100⟩ direction). The double degeneracy of the conduction band at X is removed for crystals without inversion symmetry and thus this peak should split for group III-V semiconductors. Using low-temperature (80°K) reflectivity measurements on etched single crystals, we have observed this splitting in GaAs, GaSb, InAs, and InSb. No splitting is observed in either Si or Ge. These results confirm the assignment of the main reflectivity peak in zincblende semiconductors to X transitions. The use of low temperatures, in addition to sharpening the main reflectivity peaks considerably, has revealed weak structure in all the materials studied. The general systematics of the band structure of diamond and zincblende crystals[1-4] make it possible to give reasonable assignments to nearly all of the new experimental peaks. The experimental curve for GaAs is shown in Fig. 1, and the results for the four materials are summarized in Table I.

Phillips, Ehrenreich, and Philipp[1] have given a tentative value of 0.9 eV for the X_1-X_3 gap in GaAs. However Paul has shown[5] that this splitting should be small (<0.3 eV). The value of 0.43 eV from Fig. 1 is in better agreement with this estimate. Also, the splitting for ZnSe should be double this value, and Aven, Marple, and Segall[6] have obtained a room-temperature reflectivity curve for ZnSe which clearly shows a splitting of 0.9 eV. The 8.5-eV peak in ZnSe

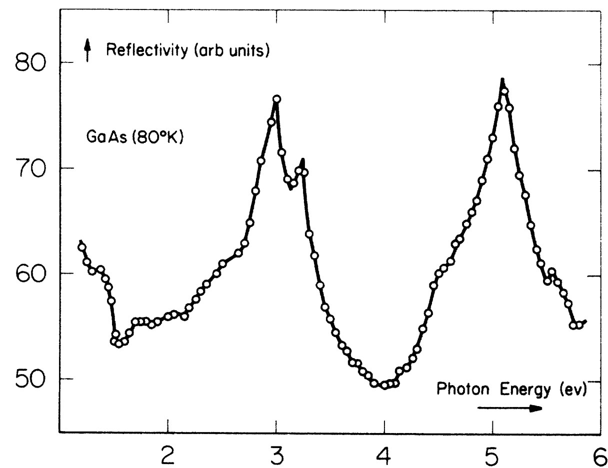

FIG. 1. Reflectivity of etched GaAs at 80°K.

Table I. Experimental reflectivity peaks in GaAs, GaSb, InAs, and InSb at 80°K between 1.2 and 6.0 eV.

	$L_3'-L_1$	$\Gamma_{25}'-\Gamma_{15}$	X_5-X_1	X_5-X_3	X_1-X_3	Other peaks
GaAs	2.99 3.23	4.2? 4.52	5.12	5.55	0.43	1.4, 1.75 = $(\Gamma_{25}'-\Gamma_2')$ 2.3, 2.6 = $(L_3'-L_1)$?
GaSb	2.08 2.55	3.74	4.33	4.70	0.37	5.7 = $(L_3'-L_3)$ 1.4, 1.9 = $(L_3'-L_1)$?
InAs	2.57 2.85	4.63	4.83	5.30	0.47	2.2, 2.45 = $(L_3'-L_1)$?
InSb	1.87 2.45	2.8? 3.45	4.20	4.70	0.50	5.4 = $(L_3'-L_3)$